Available free online at www.medjchem.com

Mediterranean Journal of Chemistry

Mediterranean Journal of Chemistry **2016**, 5(6), 599-604

Study of the pore filling fraction of carbazole-based hole-transporting materials in solid-state dye-sensitized solar cells

Marwa Ben Manaa [1,2], Safia Benhattab [1], Bruno Schmaltz[1], Nicolas Berton [1,*], Johann Bouclé [3], Abdelmottaleb Ben Lamine [2] and François Tran Van [1]

[1] Université François Rabelais, Laboratoire de Physico-Chimie des Matériaux et des Electrolytes pour l'Energie (PCM2E), EA 6299, Parc de Grandmont, F-37200 Tours, France.

[2] Unité de recherche de physique quantique, Faculté des Sciences de Monastir, Tunisia.

[3] Univ. Limoges, CNRS, XLIM, UMR 7252, F-87000 Limoges, France.

Abstract: Carbazole-based molecular glasses have emerged as a promising alternative to the widely used hole-transporting materials (HTM) spiro-OMeTAD in solid-state dye-sensitized solar cells (DSSCs). The pore filling fraction (PFF) of the mesoporous TiO_2 layer by the HTM appears as a key parameter determining the final efficiency of a DSSC. In this work, the pore-filling properties of a family of carbazole-based HTMs are investigated for the first time and the photovoltaic behavior of DSSC devices (fabricated using the D102 dye) is discussed in light of the present findings. It is found that *N*-aryl substituted 3,6-bis(diphenylaminyl)-carbazole derivatives exhibit relatively low PFF of *ca.* 60%. Methoxy groups on the diphenylamine moieties have little influence on the PFF, indicating that the strong enhancement in power conversion efficiency (PCE) is not related to an improved filling of the pores by the HTM. *N*-alkylated HTMs lead to higher PFF, increasing with the alkyl chain length, up to 78%.

Keywords: dye-sensitized solar cells (DSSC) ; hole-tansporting materials; carbazole; pore filling.

Introduction

Dye-sensitized solar cells (DSSCs) have been the focus of much attention over the past few years as they constitute a promising photovoltaic technology for the production of renewable and low-cost energy. DSSCs are usually composed of a dye-sensitized semiconducting mesoporous TiO_2 layer deposited on a transparent conducting oxide (FTO) glass substrate, a liquid electrolyte, and a counter-electrode. Molecular sensitizers, linked via anchoring groups to the oxide, inject electrons into the conduction band of the semiconductor upon light excitation, while the electrolyte containing a redox system ensures the regeneration of the photo-excited dye [1]. High power conversion efficiencies of over 13% have been reached in DSSCs [2,3]. However, leakage and corrosion issues associated with the liquid electrolyte have led to the development of solid-state DSSCs, typically using 2,2',7,7'-tetrakis-(N,N-di-*p*methoxyphenyl-amine)-9,9'-spirobifluorene (spiro-OMeTAD) as hole-transporting material (HTM) [4]. Since a few years, spiro-OMeTAD is showing increasing performances when associated with organic dyes such as D102 (4.2%) [5] or Y123 (7.2%) [6] dyes. Yet, the reference spiro-OMeTAD HTM remains still too expensive for large-scale applications and efficiencies should be improved. The development of low-cost and efficient hole-transporting materials for solid-state DSSCs is therefore a crucial challenge.

Although conjugated polymers have been considered as potential candidates due to high hole mobility and easily tunable energy levels, their use in solid-state DSSCs has been hampered because of their high molecular weight and relatively low solubility, resulting in limited penetration into mesoporous TiO_2 films, and therefore low power conversion efficiency [7]. Small molecules such as carbazole- and triarylamine-based molecular glasses are among the few emerging alternatives to spiro-OMeTAD in DSSCs as they exhibit suitable electrochemical oxidation potentials, good charge transport, thermal and morphological stability [8-12]. While the pore filling of the mesoporous TiO_2 appears to play a critical role on device efficiency in spiro-OMeTAD-containing solid-state DSSCs [13-16], there is yet a lack of data regarding the ability of the newly reported HTMs to adequately fill the TiO_2 layer. We have previously demonstrated the critical role played by methoxy groups on the phenyl moieties of carbazole-based HTMs in order to enhance the power conversion efficiency of DSSCs [9]. Although this effect was mainly attributed to charge transport properties, a positive effect on pore filling could not be excluded either, and this point

**Corresponding author: Dr. Nicolas Berton*
E-mail address: nicolas.berton@univ-tours.fr
DOI: http://dx.doi.org/

has not been addressed so far. Moreover, various studies performed by our group and others have consistently shown that *N*-aryl substituted carbazole HTMs tend to exhibit higher efficiencies in DSSCs than their *N*-alkylated analogues, but the pore filling in the devices has not been studied yet [8-10,17,18]. A better understanding of the role of the structural variations is necessary in order to design the next generation of HTMs.

The present work aims at determining the pore filling fraction (PFF) of carbazole HTMs in mesoporous TiO_2 and establishing a relationship with the photovoltaic characteristics in DSSCs. A family of four selected 3,6-bis(diphenylaminyl)-carbazole derivatives with various substituents is investigated. The results are compared with the PFF obtained for spiro-OMeTAD in similar conditions and related to the photovoltaic behavior of devices fabricated using the indoline dye D102 in FTO/TiO_2/D102/HTM/Au configuration.

Experimental Section

Sample preparation for PFF measurement

The glass substrates were cleaned by sonication in distilled water, acetone, and isopropanol. The dye-sensitized substrates were prepared following a previously reported method [9,17]. a mesoporous layer of TiO_2 was applied by spin-coating from a commercial TiO_2 paste (Astronix) containing nano-sized anatase particles, followed by gradual annealing from 250˚C up to 500˚ C, over 40 min. The resulting film thickness is *ca.* 2 µm. The substrates were then treated with 0.02 M $TiCl_4$ aqueous solution for 2 hours at room temperature, rinsed with distilled water and annealed at 500˚C for 30 min. Subsequently, they were sensitized by soaking in 0.6 mM solution of indoline D102 dye (Mitsubishi Paper Mills, Japan) in acetonitrile:*tert*-butanol (1:1 vol%, Sigma-Aldrich) overnight at 80°C and then washed with acetonitrile. The HTM layer was deposited either on a flat glass substrate or on a dye-sensitized TiO_2 substrate (1 cm^2) by spin-coating at 2000 rpm from 30 µL of the HTM solution at 200 mg/mL in chlorobenzene. The HTM solution was prepared by dissolving the HTM molecule (60 mg) in 300 µL of chlorobenzene (Sigma-Aldrich), then adding 11 µL of a $Li(CF_3SO_2)_2N$ stock solution (at 190 mg/mL in acetonitrile), and 5.3 µL of *tert*-butylpyridine. Before spin-coating, the solution was deposited onto the dye-sensitized substrates for 40 s to allow the filling of the TiO_2 pores.

Fabrication and testing of DSSCs

DSSCs were fabricated and tested as previously reported [9,17]. Gold electrodes (*ca.* 100 nm) were evaporated on top of a glass/FTO/D102-sensitized TiO_2/HTM film (prepared as described above) under vacuum (10^{-6} mbar) using shadow masks that define two active areas per substrates (0.18 cm^2 each). The current density-voltage (J-V) characteristics were recorded in air using a Keithley 2400 source-measure unit, in the dark and under simulated solar emission (Atlas Solarconstant 575PV) at a scan rate of 250 mV/s. The spectral mismatch between the emission of the solar simulator and the global AM1.5G solar spectrum (ASTM G173-03) was corrected using a mismatch factor [18] and the solar simulator irradiance was adjusted accordingly using a certified silicon reference cell in order to achieve an equivalent AM1.5G irradiance of 1 sun (100 $mW.cm^{-2}$) on the tested cells.

Results and Discussion

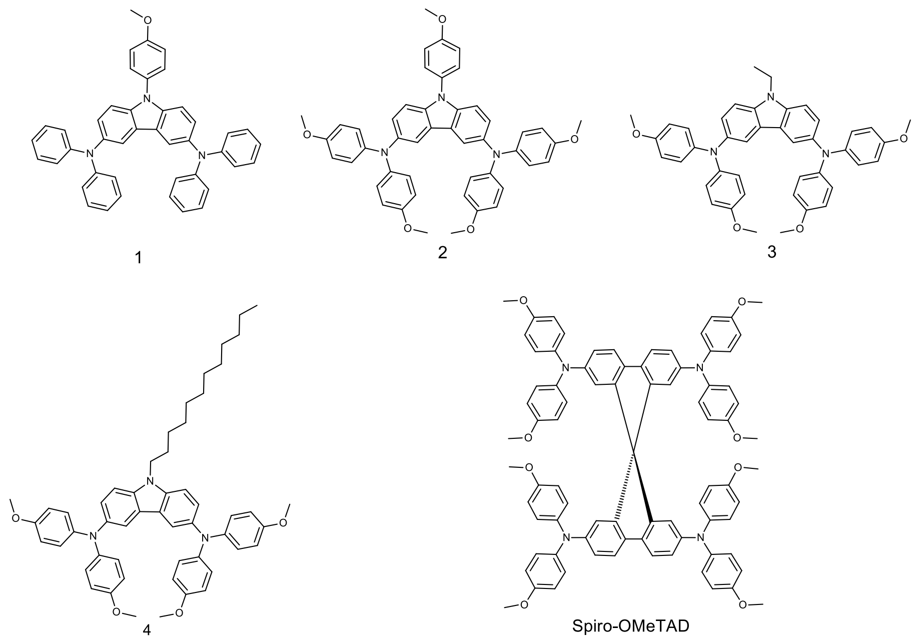

Scheme 1. Chemical structure of the studied HTMs.

Scheme 1 presents the structure of the carbazole-based hole-transporting materials used in this study along with the standard HTM molecule spiro-OMeTAD. The PFF of a family of four different carbazole-based molecular glasses is investigated by changing either the presence of the methoxy groups in para position of the diphenylamine group or the nature of the substituent (alkyl, aryl) linked to the nitrogen of the carbazole (9-position). HTMs **1**, **2** and **3** have been prepared as reported by our group [9,17]. HTM **4** was synthesized in a one-step reaction from *N*3,*N*3,*N*6,*N*6-tetrakis(4-methoxy-phenyl)-9-H-carbazole-3,6-diamine[10] via deprotonation and *N*-alkylation with 1-bromododecane on the carbazole moiety (75% yield).

The PFF of the HTM in mesoporous TiO_2 was estimated using a method previously reported in the literature [14,20]. HTM films were deposited both on a flat glass substrate and on a dye-coated porous TiO_2 substrate by spin-coating, following the procedures described in the experimental section. Before spin-coating, the HTM solution deposited onto the dye-sensitized substrates was allowed to fill the TiO_2 pores for 40 seconds. It is assumed that at the beginning of the spin-coating, a solution layer of uniform thickness (t_{wet}) is formed above the mesoporous substrate prior to solvent evaporation. As the solvent evaporates on top during spin-coating, a concentration gradient is created within the film and more HTM diffuses into the TiO_2 pores. At some critical concentration, the infiltration is likely to stop due to gelification or precipitation of the HTM. After solvent evaporation, a dry HTM overlayer remains on top of the infiltrated TiO_2 layer, as depicted in Figure 1. Therefore, the pore filling fraction (PFF) is calculated according to the following equations [20]:

$$PFF = \frac{t_{HTM}}{p \times t_{TiO_2}} \quad (1)$$

$$t_{HTM} = C \times (t_{wet} + (p \times t_{TiO_2})) - t_{overlayer} \quad (2)$$

where p is the porosity of the TiO_2 layer, t_{TiO2} is the thickness of the mesoporous TiO_2 layer, C is the %volume concentration of the HTM in the deposition solution (calculated using the experimentally determined HTM density), $t_{overlayer}$ is the dry HTM overlayer thickness and t_{wet} is the wet solution layer thickness obtained by the ratio t_{flat}/C. The TiO_2 porosity is assumed to be 60%, which is typical for mesoporous TiO_2 films. The HTM film thickness on flat glass substrate (t_{flat}), the TiO_2 thickness and the HTM capping overlayer thickness on TiO_2 ($t_{overlayer}$) were determined from cross-section SEM images (Fig. S1 and Fig. 2).

This method requires to take into account the density of the HTM in order to accurately calculate the volume concentration of the solution. In the present study, the density of the different HTMs was determined by re-dissolution of HTM films in chlorobenzene and estimation of the concentration using UV/Vis absorption spectroscopy (*cf.* Supplementary Materials) following an established procedure [15]. As evidenced in Table 1, there are only slight variations of density between the various carbazole-based molecules upon chemical structure tuning. The density remains in the 1.3-1.4 $g.cm^{-3}$ range, which is comparable with the density of the carbazole molecule (1.285 $g.cm^{-3}$) [21]. It can be noticed that the longest alkyl chain results in the highest density. Conflicting data were reported in the literature regarding the density of spiro-OMeTAD, from 1.02 $g.cm^{-3}$ [15] to 1.82 $g.cm^{-3}$ [14]. Here, we found a value of 1.90 $g.cm^{-3}$, close to the latter one.

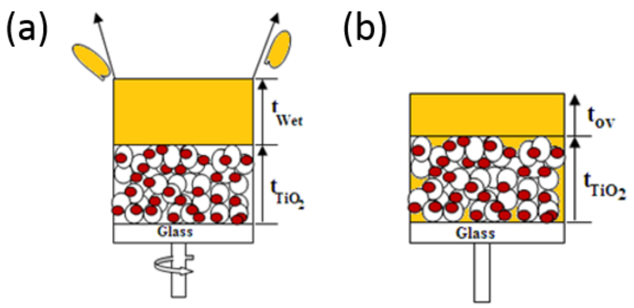

Figure 1. Schematic representation of the HTM pore filling and film forming process during spin-coating: (a) beginning of spin-coating, (b) after spin-coating.

The PFF was determined according to equations (1) and (2). Experimental measurements and calculation results are summarized in Table 1. In each case, the thickness of the TiO_2 layer was similar (*ca.* 2 µm), thus allowing to compare the ability of the different HTMs to infiltrate the mesoporous network. *N*-(4-methoxyphenyl) substituted carbazole HTMs **1** and **2** both exhibit relatively low PFF of 60% and 61%, respectively. It is noteworthy that the presence of methoxy groups in *para* position on the diphenylamine units only results in a very slight increase of the PFF. On the contrary, the pore filling is very sensitive to the nature of the *N*-substituent on the carbazole moiety. Replacing the methoxyphenyl substituent by an ethyl chain leads to a significant

PFF enhancement from 61% up to 67% with HTM **3**, compared with HTM **2**. The PFF can be further increased when the length of the alkyl chain increases, up to 78% for HTM **4** that is bearing a C_{12} linear alkyl chain. This value slightly outperforms the 75% PFF measured using spiro-OMeTAD, and represents a strong improvement in pore filling compared with the *N*-aryl substituted carbazole HTMs **1** and **2**. Thus, the incorporation of alkyl chains appears to facilitate the infiltration of the HTM into the mesoporous structure of TiO_2. Since alkyl chains bring additional solubility to organic compounds, this can be attributed to a delayed precipitation of the HTM inside the pores.

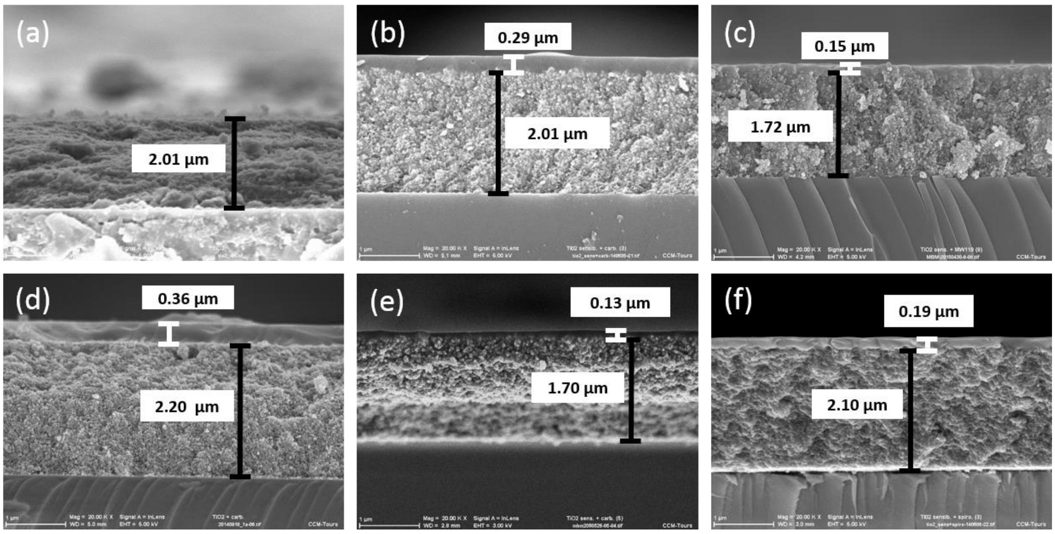

Figure 2. Cross-section SEM images of (a) TiO_2, (b) TiO_2/HTM 1, (c) TiO_2/HTM 2, (d) TiO_2/HTM 3, (e) TiO_2/HTM 4, and (f) TiO_2/spiro-OMeTAD films on glass substrate.

Table 1. Summary of HTM density, measured film thickness values and calculated pore filling fraction.

	Density (g/cm^3)	C (vol%)	t_{flat} (μm)	t_{TiO2} (μm)	$t_{overlayer}$ (μm)	PFF (%)
HTM 1	1.32	13.2	0.86	2.01	0.29	60
HTM 2	1.28	13.5	0.65	1.72	0.15	61
HTM 3	1.29	13.4	1.07	2.20	0.36	67
HTM 4	1.42	12.4	0.80	1.70	0.13	78
Spiro-OMeTAD	1.90	9.5	1.03	2.10	0.19	75

In order to investigate the influence of the pore filling on the photovoltaic performances, solid-state DSSCs were built with the novel compound HTM **4** using the device structure FTO/TiO_2/D102/HTM/Au, and the photocurrent-voltage (*J-V*) characteristics were recorded under standard 100 $mW.cm^{-2}$ AM 1.5G illumination (Fig. S2). The photovoltaic parameters are listed in Table 2 along with those recently reported by our group for devices fabricated and tested under similar conditions using HTMs **1**, **2** and **3** as well as spiro-OMeTAD [9,17]. The power conversion efficiency of the devices incorporating HTM **1** is extremely low (0.12%). Based on the present finding that the PFF is comparable for both compounds, it is evidenced that the strong improvement in efficiency observed with HTM **2** (1.75%) cannot be attributed to a better pore filling. Thus, the enhanced photovoltaic behavior is most likely related to the dye/HTM structural compatibility and/or higher hole mobility of HTM **2**. In particular, the strong increase in short-circuit current density (J_{SC}) is consistent with an improved mobility, which is typically observed when introducing methoxy groups in *para* position on the diphenylamino moieties [22]. Also, it should be noted that the extremely high series resistance measured with HTM **1** can be partly explained by the relatively thick HTM overlayer (0.29 μm) and is likely to impact the J_{SC}. In order to improve the PFF without increasing the overlayer thickness, further soaking time and spin-coating speed optimization may be required [23].

Although higher power conversion efficiencies could be expected when the PFF increases [14-16], the devices containing *N*-alkylated compounds HTM **3** and HTM **4** only exhibit efficiencies of 0.82% and 0.18%, respectively. Here, the pore filling is obviously not the main limiting factor. Performances of DSSCs made with HTM **3** may suffer from the very thick overlayer (0.36 μm) present on top of the mesoporous layer. Indeed, a PCE of 1.6% was reported for HTM **3** using an optimized process with a 2.3 μm TiO_2 thickness [18]. Interestingly, it can be noticed that HTM **3** affords the highest fill factor, consistently with the fact that a better pore filling is likely to favor hole extraction from the dye and therefore help reducing interfacial charge recombination. The low efficiency obtained for HTM **4** despite a relatively fair PFF of 78% and a reasonable overlayer thickness (0.19 µm) clearly indicates that a long linear alkyl chain has a detrimental effect on device behavior. This may be related to a drop in hole mobility as suggested by the high series resistance. There must therefore be an optimal chain length in-between C_2 and C_{12}, as is also suggested by the slight increase up to 1.8% noticed when using an hexyl chain instead of an ethyl one [18]. Yet, further structural variations, such as introducing branched alkyl chains or *N*-aryl units functionalized with alkyl or alkoxy chains for instance, will most likely be necessary to reach high pore filling while retaining the electronic properties of the HTM.

Table 2. Summary of the photovoltaic parameters of solid-state DSSCs made using the different HTMs.

	Jsc (mA/cm^2)	*Voc* (V)	FF (%)	Rs (Ω)	Rsh (Ω)	PCE (%)	Ref.
HTM 1	0.32	0.86	44	4429	49722	0.12	[9]
HTM 2	6.32	0.68	41	301	2502	1.75	[9]
HTM 3	2.68	0.65	47	413	8478	0.82	[17]
HTM 4	0.94	0.58	32	1900	5057	0.18	
Spiro-OMeTAD	7.64	0.79	59	150	34499	3.54	[9]

Conclusion

In summary, the pore filling properties of four different *N*-substituted 3,6-bis(diphenylaminyl)-carbazole derivatives were investigated for the first time. It is found that methoxy groups in *para* position on the diphenylamine moieties have little influence on the PFF, indicating that the strong enhancement in DSSC power conversion efficiency (PCE) induced by those groups is not related to an improved filling of the mesoporous TiO_2. *N*-aryl substituted carbazole HTMs exhibit relatively low PFF of *ca.* 60%. *N*-alkylated analogue HTMs lead to higher pore filling up to 78% with the longest alkyl chain (C_{12}), compared with the 75% determined for spiro-OMeTAD. Although the DSSC efficiency drops at the same time, it is demonstrated that the pore filling can be efficiently improved *via* fine chemical structure tuning. These findings will provide valuable insights for the design of efficient carbazole-based HTMs combining good intrinsic properties and pore filling in order to be used in solid-state DSSCs as well as in the strongly expanding field of mesoscopic perovskite solar cells.

Supplementary Materials

Supplementary Materials including experimental procedures, cross-section SEM images of HTM thin films on glass and *J-V* characteristics is available.

Acknowledgements

This research was funded by the Région Centre, the Tunisian ministry of research and the University of Monastir. J. Bouclé acknowledges Région Limousin and the Sigma-Lim LabEx environment for financial supports.

References

1 - B.C.O. Regan and M. Grätzel, Nature, **1991**, 353, 737-740.
2 - A. Yella, H.W. Lee, H.N. Tsao, C. Yi, A.K. Chandiran, M.K. Nazeeruddin, E.W. Diau, C.Y. Yeh, S.M. Zakeeruddin and M. Grätzel, Science, **2011**, 334, 629-634.
3 - S. Mathew, A. Yella, P. Gao, R. Humphry-Baker, F.E. Curchod Basile, N. Ashari-Astani, I. Tavernelli, U. Rothlisberger, K. Nazeeruddin and M. Grätzel, Nature Chemistry, **2014**, 6, 242-247.
4 - U. Bach, D. Luppo, P. Compte, J. Moser, E.F.Weissortel, J. Salbeck, H. Spreitzer, M. Grätzel, Nature, **1998**, 395, 583-585.
5 - H. Melhem, P. Simon, L. Beouch, F. Goubard, M. Boucharef, C. Di Bin, Y. Leconte, B. Ratier, N. Herlin- Boime, J. Bouclé, Adv. Energy Mater., **2011**, 1, 908-916.
6 - J. Burschka, A. Dualeh, F. Kessler, E. Baranoff, N.L. Cevey-Ha, C. Yi, M.K. Nazeeruddin and M. Grätzel, J. Am. Chem. Soc., **2011**, 133, 18042-18045.
7 - W. Zhang, R. Zhu, F. Li, Q. Wang and B. Liu, J. Phys. Chem. C, **2011**, 115, 7038-7043.
8 - G. Puckyte, B. Schmaltz, A. Tomkeviciene, M. Degbia, J.V. Grazulevicius, H. Melhem, J. Bouclé and F. Tran Van, J. Power Sources, **2013**, 233, 86-92.
9 - M. Degbia, B. Schmaltz, J. Bouclé, J.V. Grazulevicius and F. Tran Van, Polym. Int., **2014**, 63, 1387-1393.
10 - B. Xu, E. Sheibani, P. Liu, J. Zhang, H. Tian, N. Vlachopoulos, G. Boschloo, L. Kloo, A. Hagfeldt and L. Sun, Adv. Mater., **2014**, 6629- 6634.
11- A. Michaleviciute, M. Degbia, A. Tomkeviciene, B. Schmaltz, E. Gurskyte, J.V. Grazulevicius,

J. Bouclé and F. Tran Van, J. Power Sources, **2014**, 253, 230 - 238.

12 - B. Xu, H. Tian, L. Lin, D. Qian, H. Chen, J. Zhang, N. Vlachopoulos, G. Boschloo, Y. Luo, F. Zhang, A. Hagfeldt and L. Sun, Adv. Energy Mater., **2015**, 5, 1401185.

13 - L. Schmidt-Mende and M. Grätzel, Thin Solid Films, **2006**, 500, 296-301.

14 - I.K. Ding, N. Tetreault, J. Brillet, B.E. Hardin, E.H. Smith, S.J. Rosenthal, F. Sauvage, M.Grätzel and M.D. McGehee, Adv. Funct. Mater., **2009**, 19, 2431-2436.

15 - P. Docampo, A. Hey, S. Guldin, R. Gunning, U. Steiner and H. J. Snaith, Adv. Funct. Mater., **2012**, 22, 5010-5019.

16 - C.T. Weisspfennig, D.J. Hollman, C. Menelaou, S.D. Stranks, H.J. Joyce, M.B. Johnston, H.J. Snaith and L.M. Herz, Adv. Funct. Mater., **2014**, 24, 668-677.

17 **-** M. Degbia, M. Ben Manaa, B. Schmaltz, N. Berton, J. Bouclé, R. Antony and F. Tran Van, Materials Science in Semiconductor Processing, **2016**, 43, 90-95.

18 - T.T. Bui, S.K. Shah, M. Abbas, X. Sallenave, G. Sini, L. Hirsch and F. Goubard, ChemNanoMat, **2015**, 1, 203-210.

19 **-** J.M. Kroon, M.M. Wienk, W.J.H. Verhees and J.C. Hummelen, Thin Solid Films, **2002**, 403-404, 223-228.

20 **-** H.J. Snaith, R. Humphry-Baker, P. Chen, I. Cesar, S.M. Zakeeruddin and M. Grätzel, Nanotechnology, **2008**, 19, 424003.

21 - P.T. Clarke and J.M. Spink, Acta Cryst., **1969**, B25, 162.

22 - A. Sakalyte, J. Simokaitiene, A. Tomkeviciene, J. Keruckas, G. Buika, J.V. Grazulevicius, V. Jankauskas, C.P. Hsu and C.H. Yang, J. Phys. Chem. C, **2011**, 115, 4856-4862.

23 **-** H.S. Kim, C.R. Lee, I.H. Jang, W. Kang and N.G. Park, Bull. Korean Chem. Soc., **2012**, 33, 670-674.